Osteoarthritis-related nociceptive behaviour following mechanical joint loading correlates with cartilage damage

F. ter Heegde[1,2], A.P. Luiz[2], S. Santana-Varela[2], R. Magnusdottir[1], M. Hopkinson[1], Y. Chang[3], B. Poulet[4], R.C. Fowkes[5], J.N.Wood[2], C. Chenu[1]

[1]Skeletal Biology Group, Comparative Biomedical Science, Royal Veterinary College, London NW1 0TU, UK

[2]Molecular Nociception Group, Wolfson Institute for Biomedical Research, University College London, London WC1E 6BT UK

[3]Research Office, Royal Veterinary College, London NW1 0TU, UK

[4]Muscoskeletal Biology, Institute of Ageing and Chronic Disease, University of Liverpool, Liverpool L69 3BX, UK

[5]Endocrine Signalling Group, Comparative Biomedical Science, Royal Veterinary College, London NW1 0TU, UK

Contact details:

F. ter Heegde (freijaterheegde@gmail.com), A.P. Luiz (a.luiz@ucl.ac.uk), S. Santana-Varela (s.santana@ucl.ac.uk), R. Magnusdottir (rmagnusdottir@rvc.ac.uk), M. Hopkins (mhopkinson@rvc.ac.uk), Y. Chang (ychang@rvc.ac.uk), B. Poulet (b.poulet@liverpool.ac.uk), R.C. Fowkes (rfowkes@rvc.ac.uk), J.N.Wood (j.wood@ucl.ac.uk), C. Chenu (cchenu@rvc.ac.uk)

Corresponding author:

Chantal Chenu

The Royal Veterinary College

Royal College Street

London

NW1 0TU

United Kingdom

+44 (0)20 74685045

cchenu@rvc.ac.uk

Running title: MJL-induced pain and cartilage damage

Abstract

Objective: In osteoarthritis (OA), the pain-structure relationship remains complex and poorly understood. Here, we used the mechanical joint loading (MJL) model of OA to investigate both knee pathology and nociceptive behaviour.

Design: MJL was used to induce OA in the right knees of 12-week-old male C57BL/6 mice (40 cycles, 9N, 3x/week for two weeks). Mechanical sensitivity thresholds and weight-bearing ratios were measured before loading and at weeks one, three and six post-loading. At these time points, separate groups of loaded and non-loaded mice (n=12/group) were sacrificed, joints collected, and fur corticosterone levels measured. µCT analyses of subchondral bone integrity was performed before joint sections were prepared for nerve quantification, cartilage or synovium grading (scoring system from 0-6).

Results: Loaded mice showed increased mechanical hypersensitivity paired with altered weight-bearing. Initial ipsilateral cartilage lesions one-week post-loading (1.8±0.4) had worsened at weeks three (3.0±0.6, *CI*=-1.8--0.6) and six (2.8±0.4, *CI*=-1.6--0.4). This increase in lesion severity correlated with mechanical hypersensitivity development (correlation; 0.729, p=0.0071). Loaded mice displayed increased synovitis (3.6±0.5) compared to non-loaded mice (1.5±0.5, *CI*=-2.2--0.3) one-week post-loading which returned to normal by weeks three and six. Similarly, corticosterone levels were only increased at week one post-loading (0.21±0.04ng/mg) compared to non-loaded controls (0.14±0.01ng/mg, *CI*=-1.8--0.1). Subchondral bone integrity and nerve volume remained unchanged.

Conclusions: Our data indicates that although the loading induces an initial stress reaction and local inflammation, these processes are not directly responsible for the nociceptive phenotype observed. Instead, MJL-induced allodynia is mainly associated with OA-like progression of cartilage lesions.

Key words: Osteoarthritic pain, cartilage lesions, synovitis, knee innervation, bone integrity, stress

Introduction

Osteoarthritis is typically recognized as a degenerative joint disease characterized by a loss of cartilage. Although much of the aetiology remains unknown, the approach to understanding OA has evolved from being cartilage focussed to a more multifactorial, whole joint view of the disease [1]. The identification of pathologies in multiple joint tissues and their subsequent involvement in OA, has bought up the question how these pathologies contribute to the clinical presentation of OA-associated pain. For the patients, it is this clinical presentation of pain that is the most problematic symptom of OA. Despite the importance of pain as a symptom of knee OA, much remains unclear about how knee pathology is associated with pain in OA [2].

The complexity of this structure-pain relationship is highlighted by epidemiological studies presenting conflicting results on the correlation between pain severity and MRI or radiograph read-outs of tissue damage. Whilst some clinical studies have shown positive correlations between pain and a variety of knee pathologies including bone marrow lesions [3-7], synovitis [3, 8], effusion [4, 8, 9], cartilage degradation [6, 10-12] and meniscal tears [3], other studies show a negative or neutral correlation between pain and bone marrow lesions [9, 10], synovitis [13, 14], cartilage damage [9] or meniscal pathology [9, 10, 15, 16]. Evidently, there is currently no consensus on which single tissue pathology or combination of pathologies drives OA-associated pain. Furthermore, it is likely that the magnitude of contribution to pain severity for each tissue pathology is dependent on the stage and progression of the disease. This is then further complicated by patient-specific factors such as genetics, age and sex which, in part, can explain the discordance in patient association studies.

Animal models of OA, such as the MJL, can be used to address temporal questions regarding the development of knee pathology in correlation to OA-associated pain. Mechanical loading of the knee joint is a novel, non-invasive murine model of OA. This model induces OA by intermittent, repetitive loading of the tibia through the knee and ankle joints. Originally, this model has been used to investigate the osteogenic effect of mechanical loading on the tibia [17]. Poulet and colleagues [18] were the first to investigate the effects of different loading regimes on the knee joint. Mice sacrificed directly after two weeks of loading at 9N showed cartilage damage, osteophyte formation and meniscus pathologies combined with a thickening and fibrosis of the synovium indicative of inflammation. When mice were loaded at 9N for two weeks and sacrificed three weeks later, knee pathology analysis showed increased cartilage damage and meniscal pathology whilst the osteophyte formation remained the same and signs of synovial inflammation had decreased. Subchondral bone thickening and increased trabecular bone percentage were only seen in mice loaded at 9N for five consecutive weeks [19]. This initial

characterization of the knee pathology following loading provided the first evidence that the MJL model could be used to study OA initiation and progression in a controlled, non-invasive manner.

In previous work, we showed that the mechanical joint loading model at 9N induces a progressive and chronic pain phenotype from two weeks post-loading, characterized by the development of ipsilateral mechanical hypersensitivity, altered weight bearing and reduced mobility, without affecting thermal sensitivity [20]. Here, we used this model to gain insight into how the development of OA pathology in different tissues relates to the development of MJL-induced allodynia [20]. To this end, knee joint pathology, pain severity and animal welfare were assessed at weeks one, three and six post-loading. Pain severity was determined as the nociceptive response to von Frey hairs, taken as a measure for mechanical allodynia, and by measuring hindlimb weight bearing wherein a reduced weight borne on the ipsilateral hindlimb is indicative of increased sensitivity [21, 22]. It should be noted that, although these parameters are routinely used for assessing nociception in murine OA-related pain models [23-25], they are measurements of referred knee pain rather than being specific for knee nociception. Alongside behavioural measurements to evaluate pain, a total of five markers were measured at these time points to track the OA development; the severity of cartilage damage and synovitis in both ipsilateral and contralateral knees, the volume of sympathetic and sensory nerve fibres present in the ipsilateral knee, the integrity of the subchondral bone in the ipsilateral knee and the corticosterone levels in the fur as a measure for chronic stress. These read-outs of OA progression were subsequently correlated to behavioural read-outs to determine which pathologies matched the MJL-induced pain phenotype.

Method

Naïve, male 10-week-old C57bl/6 mice (Charles River, Oxford, UK) were housed in groups of four in individually ventilated cages and fed a standard RM1 maintenance diet *ad libitum*. All experiments were carried out in compliance with the Animals (Scientific Procedures) Act (1986) and approved by the College's Ethics and Welfare Committee and UK Home Office.

Osteoarthritis was induced in the right knee of 12-week-old mice by a two-week loading regime using an electronic testing machine (Bose 3100; TA instruments), as described previously [18, 20]. Briefly, the tibia was positioned vertically between two custom-made cups to fixate the knee and ankle joint in deep flexion of 45°. Axial compressive loads were applied to the knee joint via the upper loading cup controlled by software delivered by the loading system (WinTest7 Bose). One loading cycle consisted of 9.9 seconds holding time with a load magnitude of 2N after which a peak load of 9N was applied for 0.05sec. This 10 second trapezoidal wave loading cycle is repeated 40 times within one loading episode. These loading episodes were applied three times per week, performed on alternating days, for two consecutive weeks. The left hindlimb was left unloaded. No other experiments were performed on the mice during the two weeks of loading.

Osteoarthritis was induced in a total of 36 mice. Another 36 cage- and age-matched mice did not undergo loading but were subjected to anaesthesia and served as the non-loaded controls. Separate groups of loaded mice and non-loaded controls were sacrificed at one-, three- and six-weeks post-loading to conduct post-mortem analysis (n=2 per condition and time point). Behaviour was measured before loading (week -3) after which development of nociception was verified at weeks one, three and six post-loading, a day before the sacrifice time-point. Behavioural analysis conducted included von Frey measurements in both hindlimbs to measure mechanical sensitivity thresholds and weight bearing to measure asymmetry in stance. Researchers performing behavioural testing were blinded to the condition of the mice.

At each time point, post-mortem samples were collected for analysis. Half of the samples were used for µCT analysis, OA and synovitis grading (n=6/group) whilst the other half were used for nerve analysis (n=6/group). Hindlimbs used for µCT analysis, synovitis and OA grading were collected directly after sacrifice, post-fixed (4% formalin) and stored at 4ºC. These samples were first scanned using the µCT after which they were processed for paraffin embedding and grading. Cartilage integrity was scored using the Osteoarthritis Research Society International grading system (range 0–6) [26] whilst synovitis was scored using the six-point grading system as described by Lewis and colleagues [27]. Hindlimbs collected for nerve analysis were perfused (12,5% picric acid, 4% formalin fixative) dissected out on ice, post-fixed, decalcified and then stored in sucrose solution at -20ºC [28]. Immunocytochemistry was

used to identify sensory and sympathetic nerves [29] using primary antibodies against calcitonin gene-related peptide (CGRP) and tyrosine hydroxylase (TH), respectively. Finally, the fur was collected from all animals to analyse the corticosterone levels as a measure for chronic stress.

Extended methods for both the behavioural measurements and the post-mortem analysis can be found in the supplementary methods.

Data were analysed using GraphPad Prism (7.04). Results are presented as mean±SD. Mice were assigned conditions in a pseudo-random order, ensuring comparable behavioural baseline values and allocating different conditions within the home cage. Repeated behavioural measurements were analysed using a repeated two-way ANOVA. OA pathology read-outs for loaded and non-loaded groups across time points were compared using a parametric two-way ANOVA. Homogeneity of variances was assessed using Levene's test. Normality of the residuals were evaluated by visual inspection of the histograms. In the case of a significant time, group or interaction effect, analysis was performed to identify which data points showed differences. Between group differences at specific time points or within group differences between time points are presented with the corresponding 95% confidence interval (CI) of the difference. The Spearman's rank correlation between multiple behavioural and OA pathology read-outs was calculated using R (version 5.3.1), with results presented as a heatmap. Spearman's correlation coefficients and the corresponding p-values between parameters can be found in supplementary data. For each time point, the difference between baseline and final behavioural thresholds (difference score) of the ipsilateral mechanical thresholds and weight bearing values were used. Parameters used as measures for knee pathology are all ipsilateral values. Parameters showing the clearest pattern in correlation with behaviour over time were plotted independently to visualize the progression of the behavioural parameter in relation to the knee pathology. Additionally, linear model was employed to evaluate the association between behaviours and OA pathology over time (behaviours, time, and their interaction in the model).

Results

Mice loaded at 9N developed mechanical hypersensitivity in both hindlimbs and an altered weight bearing (Fig.1). Mice sacrificed at weeks three (Fig.1B) and six (Fig.1C) showed a difference in ipsilateral mechanical threshold values between loaded mice and non-loaded controls. Non-loaded controls showed an initial drop in threshold values at week one but then recovered whilst threshold values in loaded mice further decreased at weeks three (0.175g±0.0.7g, *CI*=0.26-0.67) and six (0.140g±0.16g, *CI*=0.30-0.71) post-loading compared to baseline values (0.645g±0.29g). Contralateral mechanical hypersensitivity development was less pronounced with loaded mice showing a lower threshold level (0.205g±0.17g) compared to non-loaded mice (0.571g±0.22g, *CI*=0.14-0.59) only six weeks post-loading (Fig.1F). Alteration in weight bearing occurred alongside this development of mechanical hypersensitivity. Loaded mice sacrificed at weeks one (Fig.1G), three (Fig.1H) and six (Fig.1I) post-loading showed a significant alteration in weight bearing over time. At six weeks post-loading the difference in weight borne on the ipsilateral paw between loaded (44.13%±3.8%) and non-loaded (49.95%±5.4%, *CI*=1.80-9.93) mice was most pronounced. See supplementary Fig1 for individual behavioural values.

Following MJL, both knees showed signs of cartilage damage; in the ipsilateral knee, MJL induced mild cartilage lesions which progressively worsened over time whilst the contralateral knees of loaded mice showed cartilage damage of a lesser extent and only at six weeks post-loading (Fig.2). Non-loaded, naïve mice did not show any change in cartilage integrity over time in either knee. In the first week following MJL the maximum OA score (Fig.2A) in the ipsilateral knees of loaded mice (1.8±0.4) was higher compared to non-loaded controls (0.9±0.4, *CI*=-1.45--0.31). The lesions worsened up till three weeks post-loading (3.0± 0.3) after which they stabilized at six weeks post-loading (2.8±0.2). Summed OA scores of the ipsilateral knees (Fig.2C) show a similar advancement of OA severity with lesions progressing from week one (11.0±6.5) to three (31.3±9.0, *CI*=-30.75--9.75) and stabilizing at week six (37.1±7.9, *CI*=-36.58--15.59). Contralateral lesions develop at a later stage with maximum OA scores (Fig.2B) of loaded mice (1.8±0.7) being higher than non-loaded mice (1.0±0.0, *CI*=-1.55--0.12) at six weeks post-loading. Summed OA scores (Fig.2D) show a more progressive increase of lesions in the contralateral knees of loaded mice with values steadily increasing from week one (5.8±5.8) to three (13.8±4.6) and six (22.0±9.7) post-loading.

The synovial lining of loaded mice showed increased signs of inflammation compared to non-loaded controls in the first weeks following MJL (Fig.3). Maximum synovitis scores for the ipsilateral knees were increased in loaded animals at week one post-loading (3.6±0.2) compared to non-loaded controls (1.5±0.2, *CI*=-3.02--1.18). Following this initial inflammation, the maximum synovitis scores

progressively decreased with a mild inflammation still present at week three (2.6±0.2) and no signs of inflammation in loaded animals at week six post-loading (2±0.4). Summed synovitis scores showed the same trend, with synovitis being highest at week one and returning to normal at week six post-loading. Contralateral knees showed no sign of synovial inflammation at any time point.

Corticosterone levels in the fur of mice collected post-mortem at each time point were analysed (Fig.4). The results show increased corticosterone levels in loaded mice (0.21±0.04ng/mg) compared to non-loaded controls (0.14±0.01ng/mg, *CI*=-1.8--0.1) one week post-loading. Later time points did not show any differences between loaded mice and non-loaded controls.

The volume of both TH+ nerve fibres (Fig.5A) and CGRP+ nerve fibres (Fig.5B) remained unchanged following MJL. Upon examination of the knee sections, it was evident that innervation was most prevalent in the ligaments, menisci and periosteum. Other regions, like subchondral bone, cartilage or synovial fluid did not consistently show any presence of nerves, see supplementary Fig2. In all cases nerve density was higher in the ligaments compared to other compartments (Fig5C-H). Images of TH+ and CGRP+ nerve fibres histology (Fig.6) illustrate the differences in morphology and density between tissues. The profile of sympathetic and sensory nerve fibres was also different, with TH+ nerve fibres showing a characteristic curling around blood vessels while CGRP+ nerves typically having long, straight fibres.

The subchondral bone integrity, measured in the femur and tibia, did not show any changes between loaded and non-loaded mice over time following MJL (Tab.1). Results were analysed per condyle (data not shown) but this did not reveal any region-specific changes in subchondral bone integrity following MJL.

Correlation analysis between pathology parameters and behavioural read-outs revealed that increasing cartilage damage over time correlates significantly to an increased mechanical sensitivity following MJL (Fig.7). The correlation analysis between pain behaviours and pathology parameters (cartilage lesions, nerve volume, corticosterone levels, subchondral bone integrity and synovitis) at weeks one, three and six post-loading is shown in Fig.7A. This analysis revealed that the maximum and summed ipsilateral cartilage lesion severity following loading showed a consistent increasing positive correlation to mechanical hypersensitivity and altered weight bearing as time progressed. Whilst the other parameters measured did correlate to mechanical hypersensitivity at certain time points, these did not show a pattern over time matching the MJL-induced progression of allodynia. In contrast, the positive correlation between summed OA scores and ipsilateral mechanical threshold values increases over time (Fig.7B) with significant interaction between time and ipsilateral mechanical difference score on the summed OA scores (p=0.0038). Whilst there is no significant correlation present at weeks one

(correlation; 0.237, p=0.4824) and three (correlation; 0.478, p=0.1368) post-loading, this does develop at week six post-loading (correlation; 0.729, p=0.0072). The calculated correlations and corresponding p-values per parameter can be found in the supplementary data.

Discussion

We have previously shown that the mechanical joint loading can be used as an appropriate model to measure OA-induced allodynia in mice [20]. Here we show that the increasing cartilage damage following MJL matches the development of nociceptive behaviour, resulting in a positive correlation between behavioural read-outs and severity of cartilage lesions six weeks post-loading. Furthermore, we show that the other parameters of OA pathology measured did not show a clear pattern in their correlation to the pain phenotype. The synovium showed signs of mild inflammation directly after loading but this returned to normal as both cartilage lesions and nociceptive behaviour started to develop. Likewise, stress levels, as indicated by fur corticosterone levels, are increased in the first week following MJL but return to normal in weeks three and six post-loading. Bone integrity and knee innervation were not altered by MJL. These findings provide a first step into understanding the pain-structure relationship in the MJL model of knee OA.

MJL induces cartilage damage in the ipsilateral joint directly after loading whilst contralateral lesions develop at a later stage. In accordance with literature [18, 20], these initial ipsilateral lesions induced by the two-week loading regime progress and worsen over three weeks after which the severity of cartilage damage stabilizes. Importantly, the time frame of lesion progression matches the development of allodynia resulting in a positive correlation between cartilage damage and mechanical hypersensitivity. Interestingly, onset of contralateral mechanical hypersensitivity also corresponds to the development of cartilage damage. Contralateral behavioural and cartilage changes, however, are only seen six weeks post-loading whereas ipsilateral changes occur from three weeks. This contralateral phenotype could result from compensatory behaviour with ipsilateral allodynia inducing altered gait and an overuse of the contralateral limb. Although these results suggest a role for cartilage degradation in the development of OA-induced nociception, the combination of both ipsilateral and contralateral phenotypes could also be indicative of central hypersensitization, comparable to that seen in patients with OA [30]. Neuroplastic centralization of pain could, in part, explain the disconnect seen between structural damage and pain severity [31] as centralized pain following OA will also be present in the absence of structural damage [32]. Nevertheless, the link between cartilage damage and nociceptive behaviour has been shown in both preclinical [33, 34] and clinical studies [10, 31]. Driscol et al. [35], showed that the severity of cartilage damage at the onset of nociception is comparable in two different surgical models of OA; the destabilization of the medial meniscus (DMM) and the partial meniscectomy (PMX) surgery. In the MJL model, the same severity of cartilage damage is seen three weeks post-loading at onset of nociceptive behaviour. The link between cartilage damage and pain is further supported by correlation studies that work to minimize between patient confounding. These show that multiple measures for pain perception correlate to joint space narrowing as a measure for cartilage

degradation [12]. Together these results suggest that cartilage damage could, at least in part, be responsible for both OA pain in patients and allodynia in animal models of OA.

Further histological analysis of the synovial lining revealed that the initial signs of synovitis present one week post-loading decrease at three weeks and are no longer present when nociceptive behaviour is established at six weeks. Although osteoarthritis is generally thought to be non-inflammatory, it has been suggested that subclinical synovitis may play a role in the early stages of OA [36]. Following the MJL-induced trauma, debris from the degrading cartilage is released into the synovium and it is possible that cells in the synovial membrane react to these pro-inflammatory mediators causing local inflammation [37, 38] thus explaining the initial inflammation. These signs of inflammation, however, decrease as the behavioural phenotype develops indicating that joint inflammation might not be directly responsible for the allodynia seen in this model. This matches with surgical models of OA pain where, after an initial inflammatory post-surgery phase, joint inflammation subsides whilst nociceptive behaviour persists [39, 40]. Furthermore, there is no upregulation of inflammatory markers in the joints of mice undergoing either DMM or PMX at the point of nociception onset [35]. Instead, in both *in vivo* and *in vitro* models, mechanically damaged chondrocytes produce pain-sensitizing molecules like nerve growth factor, bradykinin receptors B1/B2, tachykinin, and tachykinin receptor 1 [35]. The development of nociceptive behaviour following mechanical loading further supports the suggestion that mechanical injury, rather than synovitis, could drive OA pain.

Corticosterone levels in the fur, as a measure for chronic stress were increased only in the first week following loading. Exposure to stress results in the release of corticosteroids via the hypothalamic-pituitary-adrenal-axis. These hormones ensure that sufficient energy is available and dampen the immune function to enable a fight or flight reaction [41]. Elevated levels of corticosterone can therefore be indicative of a stress reaction in rodents. In most cases these corticosteroids are measured in either blood or saliva. The disadvantage of being the transient nature of the data with corticosteroid levels reflecting only the hours or minutes preceding collection [42]. Corticosteroid hormones released into the blood get incorporated into hair during growth and as such, post-mortem collected hair can be used to evaluate chronic exposure to corticosteroids over time [43, 44]. The analysis of corticosterone in the fur following MJL shows that mainly the loading period itself is stressful rather than the chronic pain that develops at a later stage. It is, therefore, possible that the large variation seen in behavioural readouts in the first week following MJL is due to the increased stress in loaded animals.

Interestingly, joint innervation was not altered over time following MJL. Literature shows that intra-articular injection of complement Freud's adjuvant (CFA), which induces painful joint inflammation, leads to increased knee joint innervation and vascularization [28, 45]. This is supported by patient data showing an increase in innervation and vascularization in subchondral bone, synovium and menisci in

painful knee OA [46, 47]. Results presented here show, to a large extent, the same localization of TH+ sympathetic nerves and CGRP+ sensory nerve in ligaments, meniscus and periosteum. Notably, both TH and CGRP staining was consistently low in the subchondral bone compartment. This contradicts literature showing both innervation of bone [48] and an increase in CGRP+ nerve fibres following surgical OA induction [49-52]. It has been shown that decalcification of bone tissue reduces the immunoreactivity of the tissue [53] which could, in part, explain the absence of subchondral bone innervation seen here. Furthermore, in contrast to the CFA model, knee innervation is not increased following MJL. One explanation could be that, unlike the CFA model, MJL does not cause severe joint inflammation and as such does not induce nerve sprouting. Nevertheless, it is still possible that other MJL-induced neuronal changes are contributing to the development of allodynia. In models of OA pain neuroplastic changes are typically seen at the level of the dorsal root ganglia or spinal cord [54-57]. Additionally, there are reports showing that sensitization to pain can be due to central sensitization [58, 59] or the recruitment of silent nociceptors [60, 61], both processes that do not require a visible increase in joint innervation to induce hypersensitivity. As such, more work needs to be done to fully understand the nature and extent of neuronal contribution to MJL-induced nociception.

As with the joint innervation, MJL did not alter subchondral bone integrity. This contrasts with what has been found in knee samples from OA patients showing that bone mineral density of the subchondral bone increases as the cartilage volume decreases [62]. This cortical thickening as OA pathology progresses also been reported in different murine OA models, including the MIA model [63, 64], the DMM model [65, 66] and in the Str/Ort mice [67]. Using the MJL model we have not been able to reproduce this subchondral bone phenotype. Accordingly, when this model was originally characterized [18], changes in bone architecture were not seen in the ipsilateral knees of mice loaded for two consecutive weeks at 9N. Instead cortical thickening was only visible following five consecutive weeks of loading [19]. Possibly, the two-week loading regime used here was not severe enough to induce clear changes in subchondral bone architecture. Furthermore, results show no differences between loaded and non-loaded animals at individual time points indicating that loading at 9N does not induce an osteogenic effect. As the literature reports osteogenic effects with loading regimes at 13N or higher [17], an osteogenic effect at 9N was not expected.

The correlation analysis revealed an increasing positive correlation between MJL-induced allodynia and progressive cartilage damage over time. Interestingly, all other pathology markers measured did not show a similar pattern in correlation to MJL-induced allodynia progression. Of note is that these coefficients are dependent on the variation in the data. Groups and outcomes are, therefore, not directly comparable. As mentioned previously, the pain-structure relationship in knee OA is extremely complex and, whilst results presented add to our knowledge, much remains unknown regarding other OA-related pathologies not measured here. Literature has demonstrated the importance of tissue pathologies like

bone marrow lesions [68] or meniscal pathology [69] in the development of OA-associated pain; yet how these pathologies manifest themselves in the MJL model and if they contribute to the behavioural phenotype is unknown. Although work remains to be done to understand how cartilage damage induces nociceptive behaviour and which other tissue pathologies potentially play in OA-associated pain, these findings provide valuable insight into the pain-structure relationship in the MJL model.

Acknowledgements

This project has received funding from the European Union's Horizon 2020 research and innovation programme under the Marie Skłodowska-Curie grant agreement No 642720. Ana Paula Luiz is a fellow of Versus Arthritis UK.

Author contributions

F. ter Heegde: Conception and design; collection and assembly of data; analysis and interpretation of the data; drafting of the article; final approval of the article.
A.P. Luiz: Administrative, technical, or logistic support; collection and assembly of data.
S. Santana-Varela: Administrative, technical, or logistic support; collection and assembly of data
R. Magnusdottir: Conception and design; analysis and interpretation of the data
M. Hopkins: Administrative, technical, or logistic support; analysis and interpretation of the data
Y. Chang: Conception and design; analysis and interpretation of the data
B. Poulet: Administrative, technical, or logistic support; analysis and interpretation of the data
R. Fowkes: Administrative, technical, or logistic support; analysis and interpretation of the data; final approval of the article
J.N.Wood: Critical revision of the article for important intellectual content; obtaining of funding; final approval of the article.
C. Chenu: Conception and design; critical revision of the article for important intellectual content; obtaining of funding; final approval of the article

Role of funding source

The funders had no role in study design, data collection and analysis, decision to publish, or preparation of the manuscript.

Conflict of interest

None of the authors have any conflict of interest to disclose

References

1. Martel-Pelletier, J., et al., *Osteoarthritis.* Nat Rev Dis Primers, 2016. **2**: p. 16072.
2. O'Neill, T.W. and D.T. Felson, *Mechanisms of Osteoarthritis (OA) Pain.* Curr Osteoporos Rep, 2018. **16**(5): p. 611-616.
3. Torres, L., et al., *The relationship between specific tissue lesions and pain severity in persons with knee osteoarthritis.* Osteoarthritis Cartilage, 2006. **14**(10): p. 1033-40.
4. Lo, G.H., et al., *Strong association of MRI meniscal derangement and bone marrow lesions in knee osteoarthritis: data from the osteoarthritis initiative.* Osteoarthritis Cartilage, 2009. **17**(6): p. 743-7.
5. Felson, D.T., et al., *The association of bone marrow lesions with pain in knee osteoarthritis.* Ann Intern Med, 2001. **134**(7): p. 541-9.
6. Sowers, M.F., et al., *Magnetic resonance-detected subchondral bone marrow and cartilage defect characteristics associated with pain and X-ray-defined knee osteoarthritis.* Osteoarthritis Cartilage, 2003. **11**(6): p. 387-93.
7. Hunter, D.J., et al., *The reliability of a new scoring system for knee osteoarthritis MRI and the validity of bone marrow lesion assessment: BLOKS (Boston Leeds Osteoarthritis Knee Score).* Ann Rheum Dis, 2008. **67**(2): p. 206-11.
8. Hill, C.L., et al., *Knee effusions, popliteal cysts, and synovial thickening: association with knee pain in osteoarthritis.* J Rheumatol, 2001. **28**(6): p. 1330-7.
9. Kornaat, P.R., et al., *Osteoarthritis of the knee: association between clinical features and MR imaging findings.* Radiology, 2006. **239**(3): p. 811-7.
10. Link, T.M., et al., *Osteoarthritis: MR imaging findings in different stages of disease and correlation with clinical findings.* Radiology, 2003. **226**(2): p. 373-81.
11. Wluka, A.E., et al., *How does tibial cartilage volume relate to symptoms in subjects with knee osteoarthritis?* Ann Rheum Dis, 2004. **63**(3): p. 264-8.
12. Neogi, T., et al., *Association between radiographic features of knee osteoarthritis and pain: results from two cohort studies.* BMJ, 2009. **339**: p. b2844.
13. Hill, C.L., et al., *Synovitis detected on magnetic resonance imaging and its relation to pain and cartilage loss in knee osteoarthritis.* Ann Rheum Dis, 2007. **66**(12): p. 1599-603.
14. Pelletier, J.P., et al., *A new non-invasive method to assess synovitis severity in relation to symptoms and cartilage volume loss in knee osteoarthritis patients using MRI.* Osteoarthritis Cartilage, 2008. **16 Suppl 3**: p. S8-13.
15. Englund, M., et al., *Incidental meniscal findings on knee MRI in middle-aged and elderly persons.* N Engl J Med, 2008. **359**(11): p. 1108-15.
16. Bhattacharyya, T., et al., *The clinical importance of meniscal tears demonstrated by magnetic resonance imaging in osteoarthritis of the knee.* J Bone Joint Surg Am, 2003. **85-A**(1): p. 4-9.
17. De Souza, R.L., et al., *Non-invasive axial loading of mouse tibiae increases cortical bone formation and modifies trabecular organization: a new model to study cortical and cancellous compartments in a single loaded element.* Bone, 2005. **37**(6): p. 810-8.
18. Poulet, B., et al., *Characterizing a novel and adjustable noninvasive murine joint loading model.* Arthritis Rheum, 2011. **63**(1): p. 137-47.
19. Poulet, B., et al., *Intermittent applied mechanical loading induces subchondral bone thickening that may be intensified locally by contiguous articular cartilage lesions.* Osteoarthritis Cartilage, 2015. **23**(6): p. 940-8.
20. Ter Heegde, F., et al., *Non-invasive mechanical joint loading as an alternative model for osteoarthritic pain.* Arthritis Rheumatol, 2019.
21. Chaplan, S.R., et al., *Quantitative assessment of tactile allodynia in the rat paw.* J Neurosci Methods, 1994. **53**(1): p. 55-63.
22. Malfait, A.M., C.B. Little, and J.J. McDougall, *A commentary on modelling osteoarthritis pain in small animals.* Osteoarthritis Cartilage, 2013. **21**(9): p. 1316-26.
23. Piel, M.J., J.S. Kroin, and H.J. Im, *Assessment of knee joint pain in experimental rodent models of osteoarthritis.* Methods Mol Biol, 2015. **1226**: p. 175-81.

24. Piel, M.J., et al., *Pain assessment in animal models of osteoarthritis.* Gene, 2014. **537**(2): p. 184-8.
25. Kuyinu, E.L., et al., *Animal models of osteoarthritis: classification, update, and measurement of outcomes.* J Orthop Surg Res, 2016. **11**: p. 19.
26. Glasson, S.S., et al., *The OARSI histopathology initiative - recommendations for histological assessments of osteoarthritis in the mouse.* Osteoarthritis Cartilage, 2010. **18 Suppl 3**: p. S17-23.
27. Lewis, J.S., et al., *Acute joint pathology and synovial inflammation is associated with increased intra-articular fracture severity in the mouse knee.* Osteoarthritis Cartilage, 2011. **19**(7): p. 864-73.
28. Jimenez-Andrade, J.M. and P.W. Mantyh, *Sensory and sympathetic nerve fibers undergo sprouting and neuroma formation in the painful arthritic joint of geriatric mice.* Arthritis Res Ther, 2012. **14**(3): p. R101.
29. Chartier, S.R., et al., *Exuberant sprouting of sensory and sympathetic nerve fibers in nonhealed bone fractures and the generation and maintenance of chronic skeletal pain.* Pain, 2014. **155**(11): p. 2323-36.
30. Lluch, E., et al., *Evidence for central sensitization in patients with osteoarthritis pain: a systematic literature review.* Eur J Pain, 2014. **18**(10): p. 1367-75.
31. Pelletier, J.P., et al., *Risk factors associated with the loss of cartilage volume on weight-bearing areas in knee osteoarthritis patients assessed by quantitative magnetic resonance imaging: a longitudinal study.* Arthritis Res Ther, 2007. **9**(4): p. R74.
32. Finan, P.H., et al., *Discordance between pain and radiographic severity in knee osteoarthritis: findings from quantitative sensory testing of central sensitization.* Arthritis Rheum, 2013. **65**(2): p. 363-72.
33. Nwosu, L.N., et al., *Relationship between structural pathology and pain behaviour in a model of osteoarthritis (OA).* Osteoarthritis Cartilage, 2016. **24**(11): p. 1910-1917.
34. Tran, P.B., et al., *Spinal microglial activation in a murine surgical model of knee osteoarthritis.* Osteoarthritis Cartilage, 2017. **25**(5): p. 718-726.
35. Driscoll, C., et al., *Nociceptive Sensitizers Are Regulated in Damaged Joint Tissues, Including Articular Cartilage, When Osteoarthritic Mice Display Pain Behavior.* Arthritis Rheumatol, 2016. **68**(4): p. 857-67.
36. Mathiessen, A. and P.G. Conaghan, *Synovitis in osteoarthritis: current understanding with therapeutic implications.* Arthritis Res Ther, 2017. **19**(1): p. 18.
37. de Lange-Brokaar, B.J., et al., *Synovial inflammation, immune cells and their cytokines in osteoarthritis: a review.* Osteoarthritis Cartilage, 2012. **20**(12): p. 1484-99.
38. Sokolove, J. and C.M. Lepus, *Role of inflammation in the pathogenesis of osteoarthritis: latest findings and interpretations.* Ther Adv Musculoskelet Dis, 2013. **5**(2): p. 77-94.
39. Knights, C.B., C. Gentry, and S. Bevan, *Partial medial meniscectomy produces osteoarthritis pain-related behaviour in female C57BL/6 mice.* Pain, 2012. **153**(2): p. 281-92.
40. Inglis, J.J., et al., *Regulation of pain sensitivity in experimental osteoarthritis by the endogenous peripheral opioid system.* Arthritis Rheum, 2008. **58**(10): p. 3110-9.
41. de Kloet, E.R., M. Joels, and F. Holsboer, *Stress and the brain: from adaptation to disease.* Nat Rev Neurosci, 2005. **6**(6): p. 463-75.
42. Hellhammer, J., et al., *Several daily measurements are necessary to reliably assess the cortisol rise after awakening: state- and trait components.* Psychoneuroendocrinology, 2007. **32**(1): p. 80-6.
43. Pragst, F. and M.A. Balikova, *State of the art in hair analysis for detection of drug and alcohol abuse.* Clin Chim Acta, 2006. **370**(1-2): p. 17-49.
44. Erickson, R.L., C.A. Browne, and I. Lucki, *Hair corticosterone measurement in mouse models of type 1 and type 2 diabetes mellitus.* Physiol Behav, 2017. **178**: p. 166-171.
45. Ghilardi, J.R., et al., *Neuroplasticity of sensory and sympathetic nerve fibers in a mouse model of a painful arthritic joint.* Arthritis Rheum, 2012. **64**(7): p. 2223-32.
46. Eitner, A., et al., *The innervation of synovium of human osteoarthritic joints in comparison with normal rat and sheep synovium.* Osteoarthritis Cartilage, 2013. **21**(9): p. 1383-91.

47. Ashraf, S., et al., *Increased vascular penetration and nerve growth in the meniscus: a potential source of pain in osteoarthritis.* Ann Rheum Dis, 2011. **70**(3): p. 523-9.
48. Serre, C.M., et al., *Evidence for a dense and intimate innervation of the bone tissue, including glutamate-containing fibers.* Bone, 1999. **25**(6): p. 623-9.
49. Zhu, S., et al., *Subchondral bone osteoclasts induce sensory innervation and osteoarthritis pain.* J Clin Invest, 2019. **129**(3): p. 1076-1093.
50. Shao, Y.J., et al., *Sensory nerves protect from the progression of early stage osteoarthritis in mice.* Connect Tissue Res, 2019: p. 1-11.
51. Aso, K., et al., *Nociceptive phenotype alterations of dorsal root ganglia neurons innervating the subchondral bone in osteoarthritic rat knee joints.* Osteoarthritis Cartilage, 2016. **24**(9): p. 1596-603.
52. Obeidat, A.M., et al., *The nociceptive innervation of the normal and osteoarthritic mouse knee.* Osteoarthritis Cartilage, 2019.
53. Chartier, S.R., et al., *Immunohistochemical localization of nerve growth factor, tropomyosin receptor kinase A, and p75 in the bone and articular cartilage of the mouse femur.* Mol Pain, 2017. **13**: p. 1744806917745465.
54. Otis, C., et al., *Spinal neuropeptide modulation, functional assessment and cartilage lesions in a monosodium iodoacetate rat model of osteoarthritis.* Neuropeptides, 2017. **65**: p. 56-62.
55. Ogbonna, A.C., et al., *Pain-like behaviour and spinal changes in the monosodium iodoacetate model of osteoarthritis in C57Bl/6 mice.* Eur J Pain, 2013. **17**(4): p. 514-26.
56. Orita, S., et al., *Pain-related sensory innervation in monoiodoacetate-induced osteoarthritis in rat knees that gradually develops neuronal injury in addition to inflammatory pain.* BMC Musculoskelet Disord, 2011. **12**: p. 134.
57. Miller, R.E., et al., *Visualization of Peripheral Neuron Sensitization in a Surgical Mouse Model of Osteoarthritis by In Vivo Calcium Imaging.* Arthritis Rheumatol, 2018. **70**(1): p. 88-97.
58. Harvey, V.L. and A.H. Dickenson, *Behavioural and electrophysiological characterisation of experimentally induced osteoarthritis and neuropathy in C57Bl/6 mice.* Mol Pain, 2009. **5**: p. 18.
59. Schuelert, N. and J.J. McDougall, *Grading of monosodium iodoacetate-induced osteoarthritis reveals a concentration-dependent sensitization of nociceptors in the knee joint of the rat.* Neurosci Lett, 2009. **465**(2): p. 184-8.
60. Prato, V., et al., *Functional and Molecular Characterization of Mechanoinsensitive "Silent" Nociceptors.* Cell Rep, 2017. **21**(11): p. 3102-3115.
61. Hirth, M., et al., *Nerve growth factor induces sensitization of nociceptors without evidence for increased intraepidermal nerve fiber density.* Pain, 2013. **154**(11): p. 2500-11.
62. Bobinac, D., et al., *Changes in articular cartilage and subchondral bone histomorphometry in osteoarthritic knee joints in humans.* Bone, 2003. **32**(3): p. 284-90.
63. Mohan, G., et al., *Application of in vivo micro-computed tomography in the temporal characterisation of subchondral bone architecture in a rat model of low-dose monosodium iodoacetate-induced osteoarthritis.* Arthritis Res Ther, 2011. **13**(6): p. R210.
64. Boudenot, A., et al., *Effect of interval-training exercise on subchondral bone in a chemically-induced osteoarthritis model.* Osteoarthritis Cartilage, 2014. **22**(8): p. 1176-85.
65. Iijima, H., et al., *Effects of short-term gentle treadmill walking on subchondral bone in a rat model of instability-induced osteoarthritis.* Osteoarthritis Cartilage, 2015. **23**(9): p. 1563-74.
66. Das Neves Borges, P., T.L. Vincent, and M. Marenzana, *Automated assessment of bone changes in cross-sectional micro-CT studies of murine experimental osteoarthritis.* PLoS One, 2017. **12**(3): p. e0174294.
67. Stok, K.S., et al., *Revealing the interplay of bone and cartilage in osteoarthritis through multimodal imaging of murine joints.* Bone, 2009. **45**(3): p. 414-22.
68. Foong, Y.C., et al., *The clinical significance, natural history and predictors of bone marrow lesion change over eight years.* Arthritis Res Ther, 2014. **16**(4): p. R149.
69. Roubille, C., et al., *The presence of meniscal lesions is a strong predictor of neuropathic pain in symptomatic knee osteoarthritis: a cross-sectional pilot study.* Arthritis Res Ther, 2014. **16**(6): p. 507.

Figures

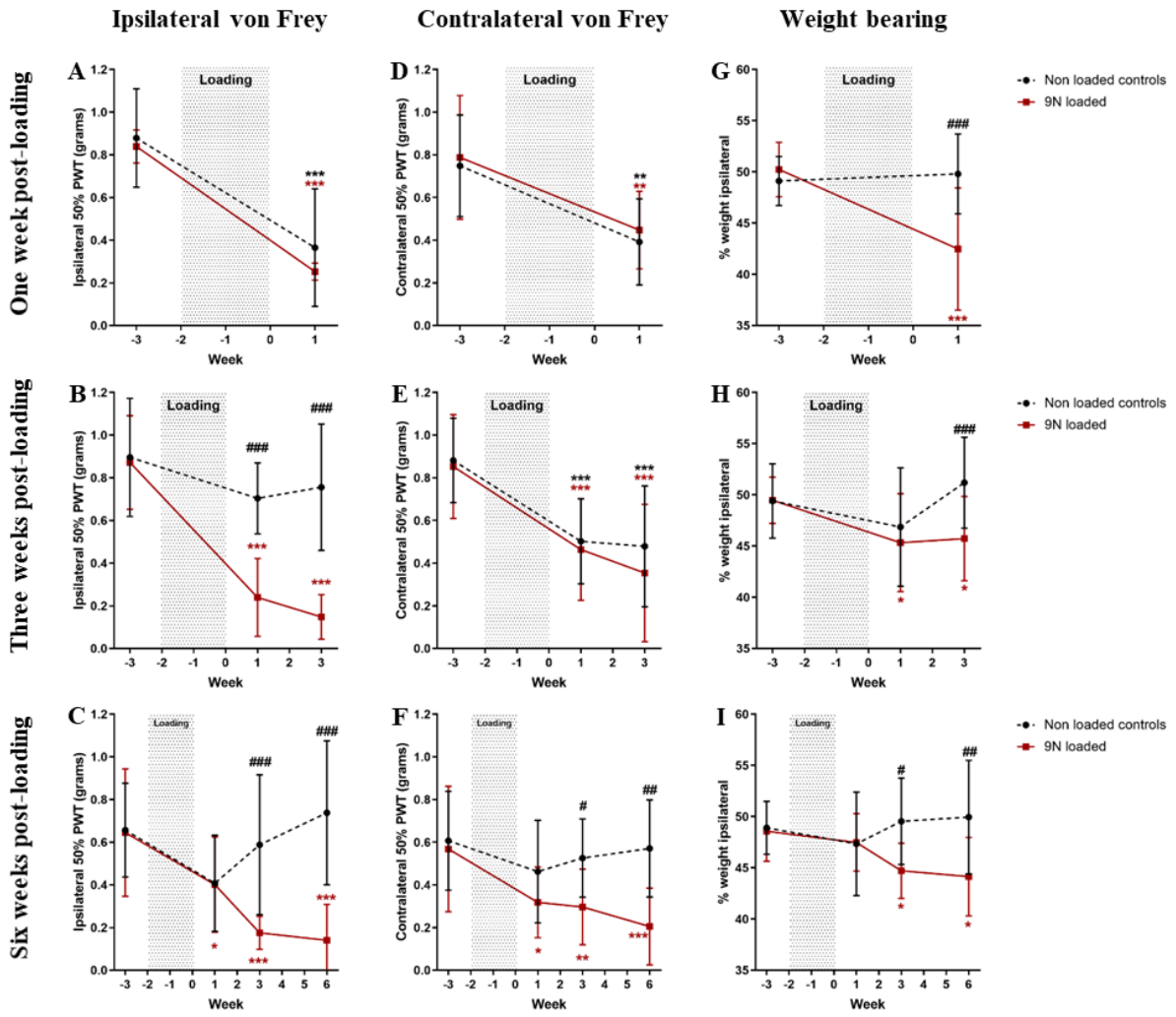

Figure 1 Development of mechanical hypersensitivity and altered weight bearing following MJL

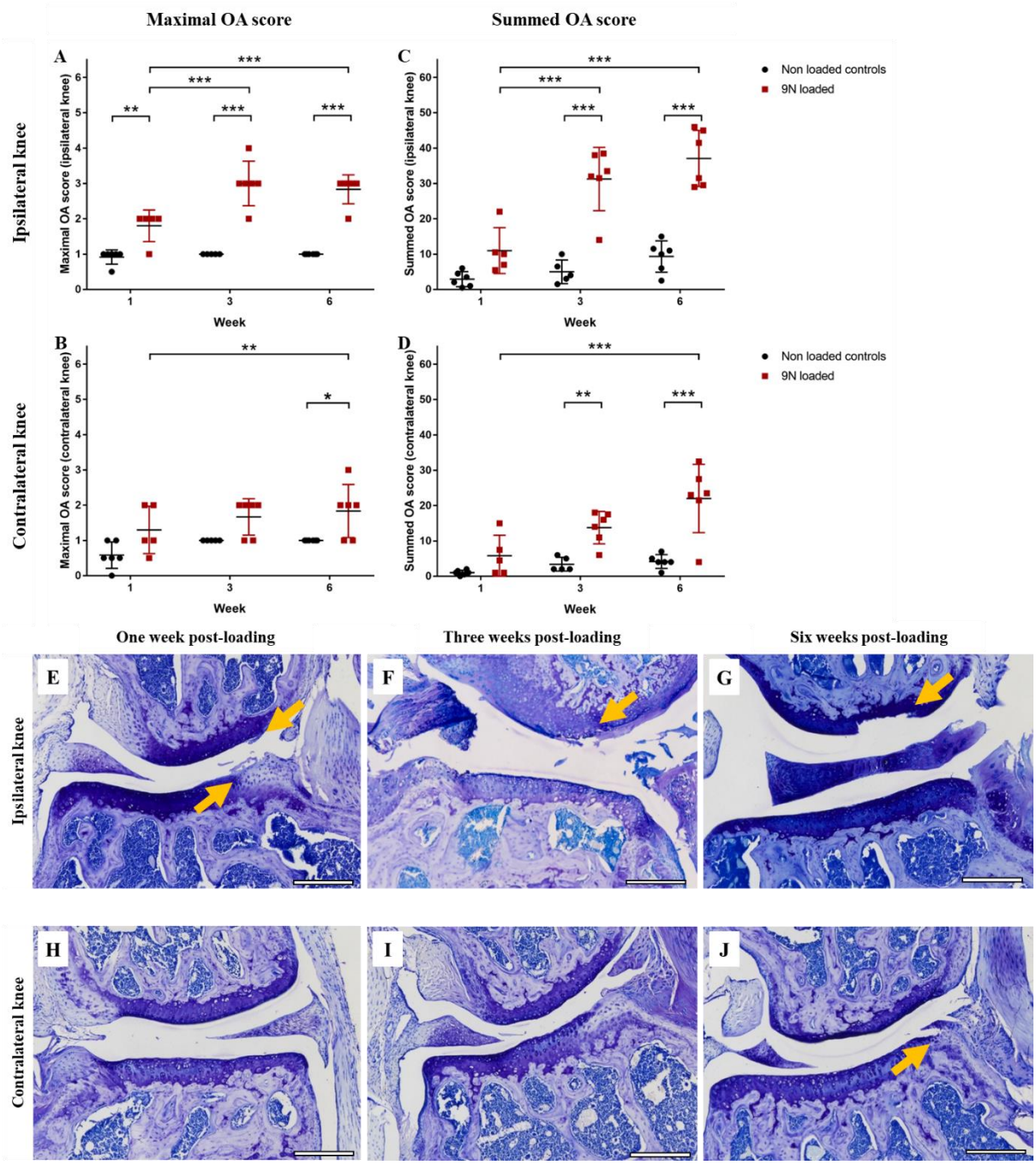

Figure 2 Severity of OA-like cartilage lesions following MJL

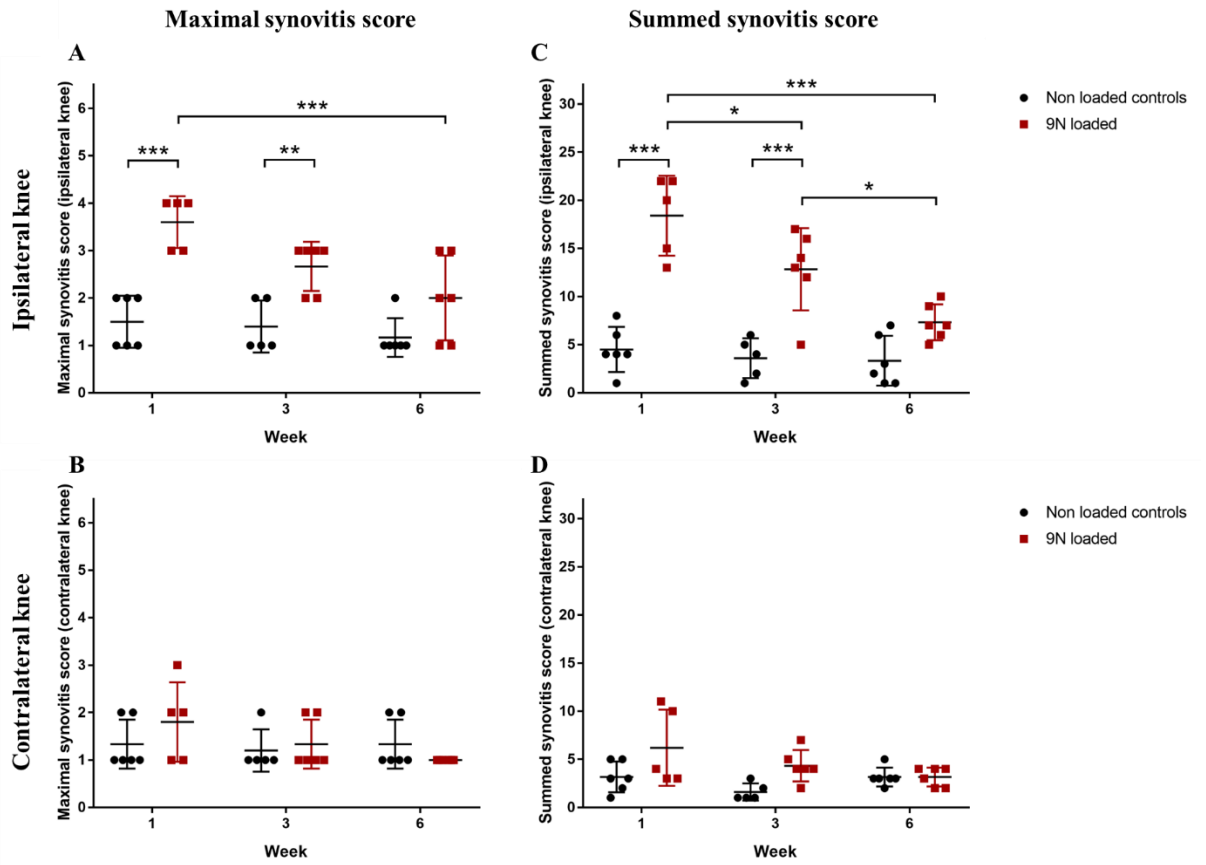

Figure 3 Severity of synovitis following MJL

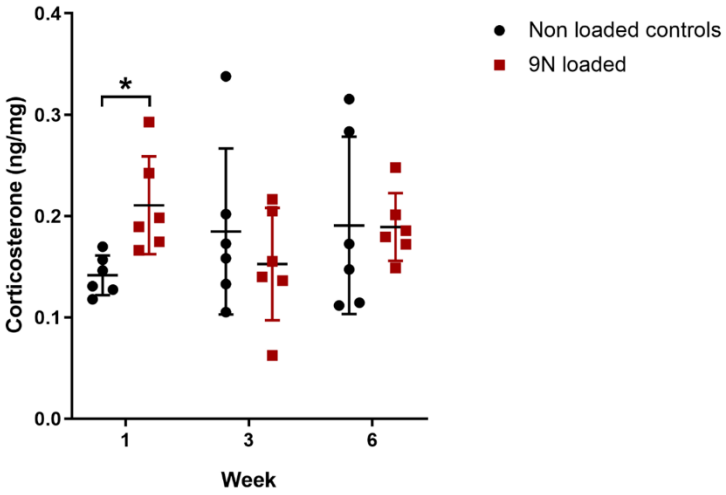

Figure 4 Corticosterone levels in the fur of loaded and non-loaded mice after MJL

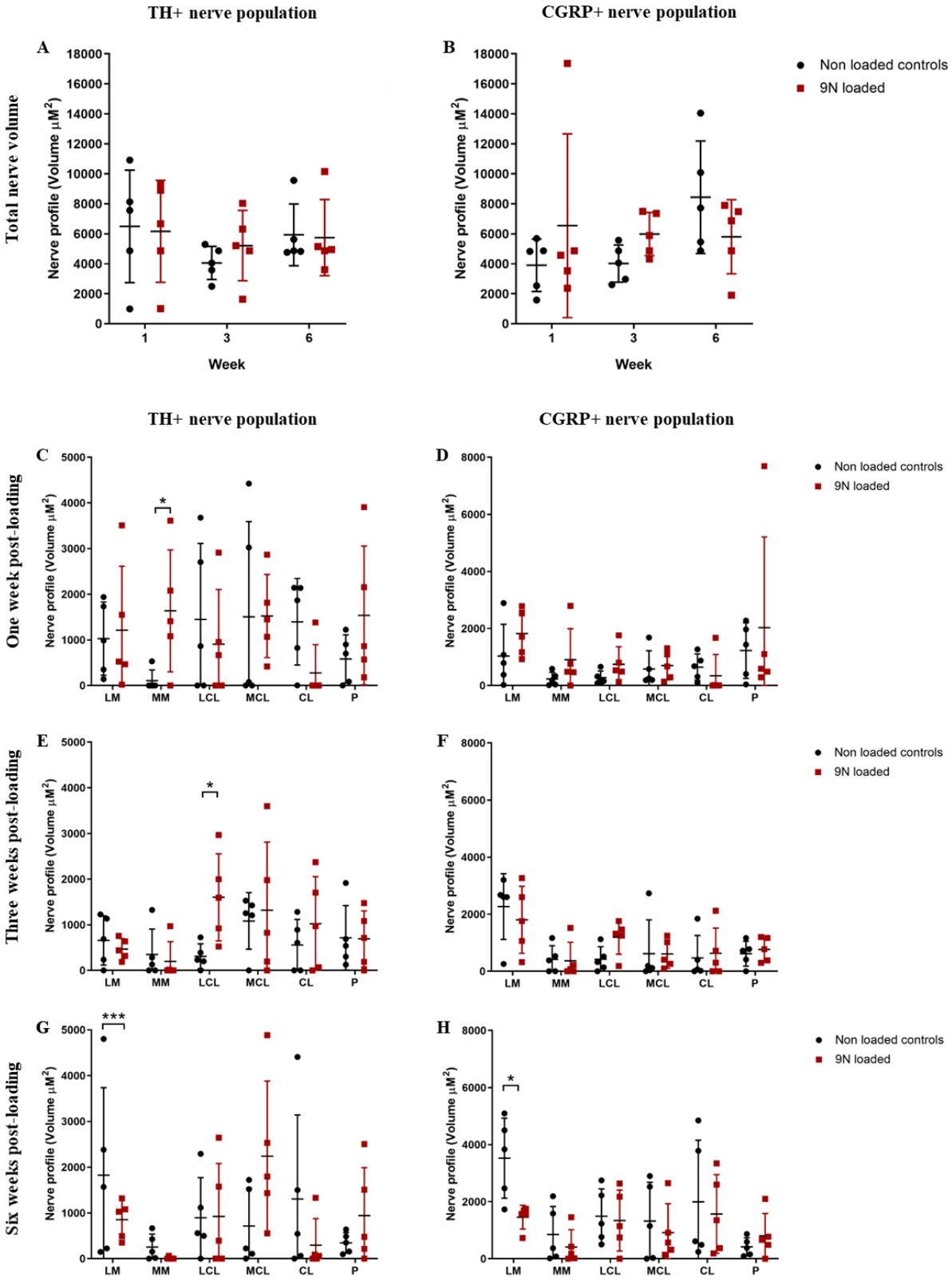

Figure 5 Tyrosine hydroxylase (TH) and calcitonin gene-related peptide (CGRP) positive nerve fibres following MJL

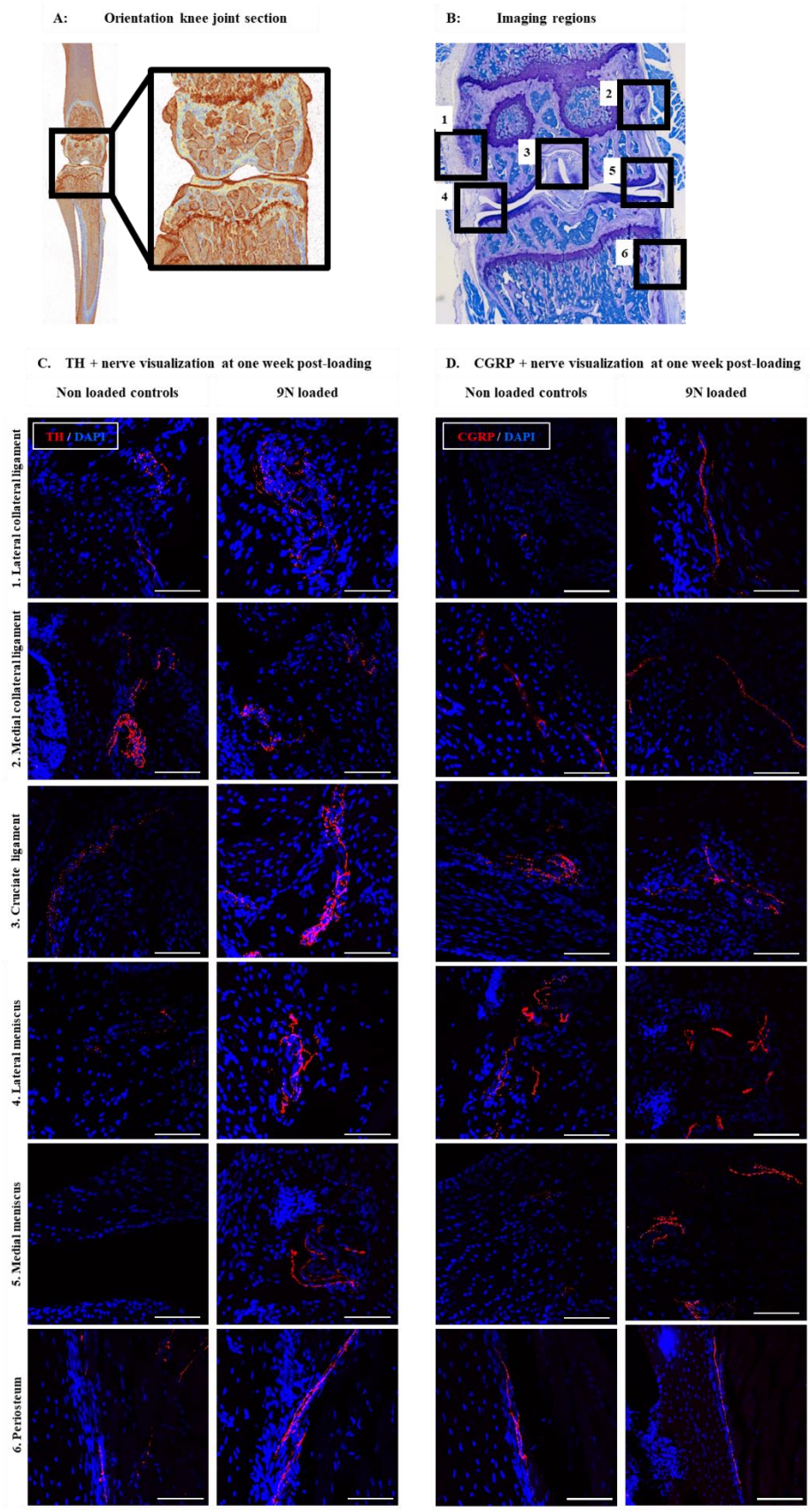

Figure 6 Visualization of TH+ and CGRP+ labelling in specified regions of the knee joint of loaded and non-loaded mice at week one following MJL

A. Overall correlation analysis between behavioural and pathological parameters

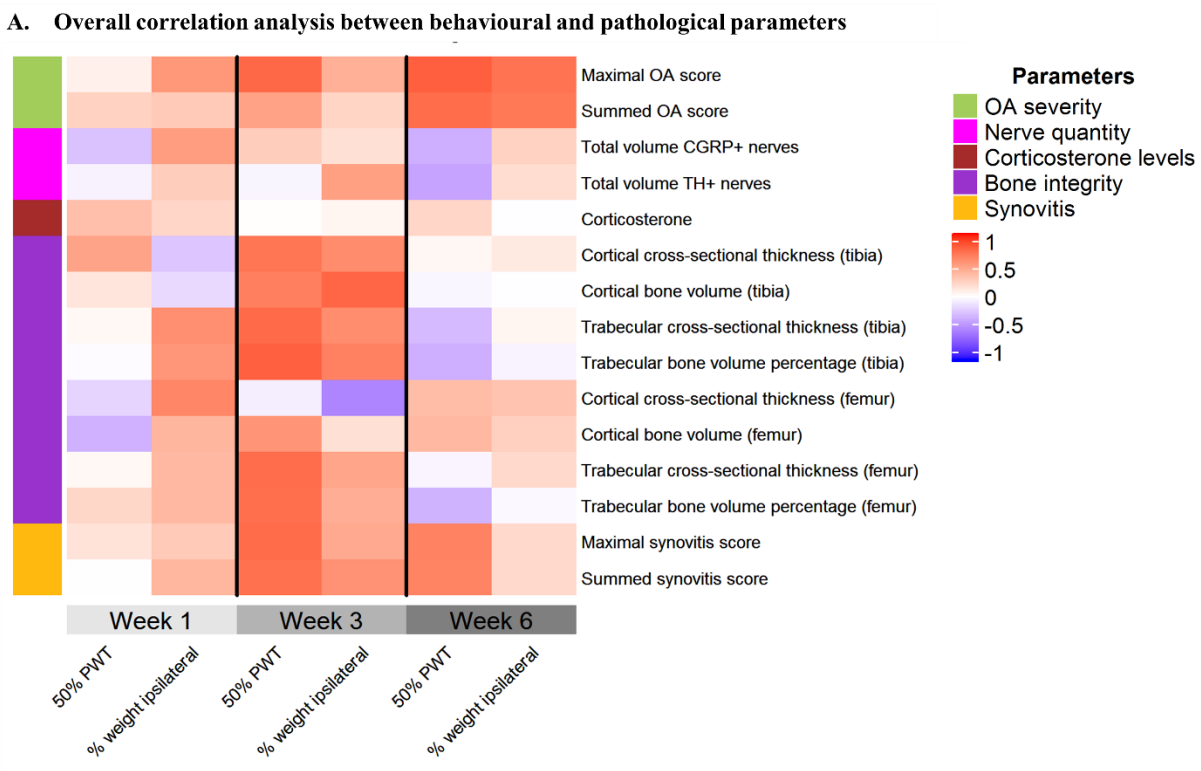

B. Correlation between summed OA score and ipsilateral mechanical hypersensitivity

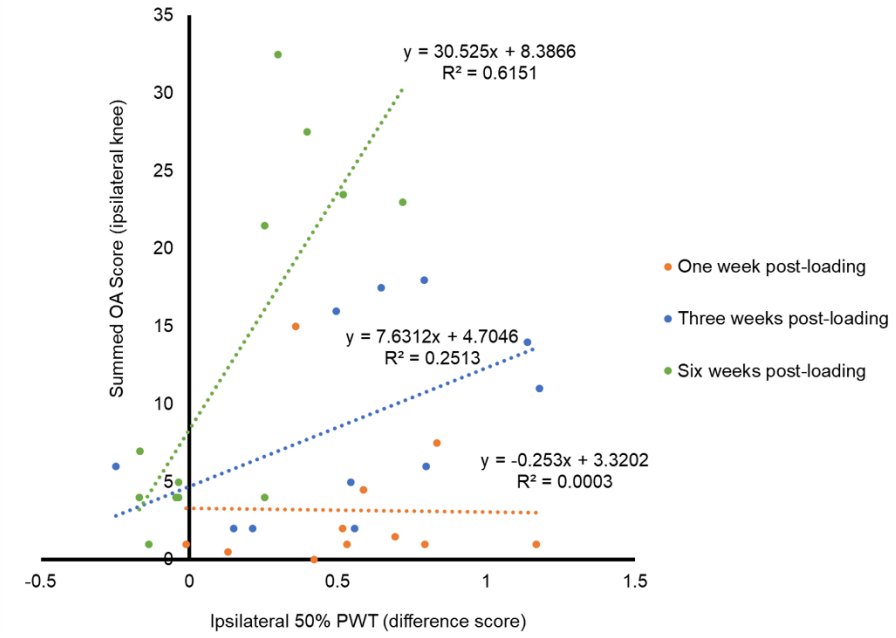

Figure 7 Correlation analysis between pain behaviours and OA parameters following MJL

Table 1 Summary µCT parameters of subchondral bone in loaded and non-loaded mice following MJL

There were no significant differences in µCT parameters between non-loaded controls and loaded mice. Values given as mean ± SEM with corresponding *p* -values.

µCT Parameter	Region of interest	Condition	One week post-loading	Three weeks post-loading	Six weeks post-loading
subchondral plate thickness (mm)	Tibia	Non-loaded control	0.052 ± 0.001	0.084 ± 0.002	0.095 ± 0.002
		Loaded	0.052 ± 0.001	0.087 ± 0.001	0.098 ± 0.003
		p – value	> 0.9999	0.7641	0.6570
	Femur	Non-loaded control	0.083 ± 0.002	0.075 ± 0.002	0.083 ± 0.002
		Loaded	0.083 ± 0.002	0.077 ± 0.001	0.088 ± 0.003
		p - value	0.9912	0.9513	0.1632
Trabecular BV/TV (%)	Tibia	Non-loaded control	43.12 ± 1.34	40.06 ± 1.87	46.77 ± 1.51
		Loaded	47.26 ± 1.85	44.98 ± 1.10	43.79 ± 2.09
		p - value	0.2271	0.1453	0.4997
	Femur	Non-loaded control	43.55 ± 1.48	40.44 ± 1.66	46.95 ± 0.94
		Loaded	45.17 ± 1.09	43.55 ± 1.28	44.68 ± 1.90
		p - value	0.8031	0.3733	0.5930
Trabecular thickness (mm)	Tibia	Non-loaded control	0.051 ± 0.002	0.050 ± 0.002	0.058 ± 0.001
		Loaded	0.054 ± 0.002	0.055 ± 0.002	0.056 ± 0.002
		p - value	0.3583	0.1313	0.6610
	Femur	Non-loaded control	0.054 ± 0.002	0.053 ± 0.002	0.062 ± 0.001
		Loaded	0.056 ± 0.001	0.057 ± 0.002	0.059 ± 0.003
		p - value	0.8462	0.4034	0.6191

Figure legends

Figure 1: Development of mechanical hypersensitivity and altered weight bearing following MJL

The right knees of mice were loaded three times per week for two weeks at 9N (red line, n = 12 per time point) to induce OA. Behavioural read-outs were compared to non-loaded isoflurane controls (black dotted line, n = 12 per time point). Mice were sacrificed at weeks one (**A, D, G**), three (**B, E, H**) and six (**C, F, I)** post-loading. Development of mechanical hypersensitivity was measured using von Frey filaments (50% paw withdrawal threshold (PWT) in grams) in the ipsilateral (**A, B, C)** and contralateral (**D, E, F**) paws. Altered weight bearing (weight placed on ipsilateral paw as a percentage of total weight placed on both legs) was measured using the incapacitance test (**G, H, I**). Differences between non-loaded and loaded animals are indicated with # ($p < 0.05$), ## ($p < 0.01$) or ### ($p < 0.001$) whilst a change within groups over time (compared to baseline value) are indicated with a * ($p < 0.05$), ** ($p < 0.01$) or *** ($p < 0.001$) in corresponding colours. Values given as the mean ± SD.

Figure 2: Severity of OA-like cartilage lesions following MJL

Ipsilateral and contralateral knees of 9N-loaded mice (red squares, n = 5-6) were collected post mortem at weeks one, three and six post-loading after which OA severity was scored for each joint section. Values were compared to non-loaded isoflurane controls (black circles, n = 5-6). Scoring system ranges from 0-6, OA severity is classified as either low (grade 0-2), mild (grade 3-4) or severe (grade 5-6). For each sample, maximum scores (**A**; ipsilateral knees, **B**; contralateral knees), determined as the lesions with the highest severity, and summed scores (**C**; ipsilateral knees, **D**; contralateral knees) are given. Differences in the severity of OA lesions between groups are indicated with a * ($p < 0.05$), ** ($p < 0.01$) or *** ($p < 0.001$). Values given as mean ± SD. Representative images of toluidine blue stained, coronal knee sections are shown for the ipsilateral knee at one (**E**), three (**F**) and six (**G**) weeks post-loading as for the contralateral knee at at one (**H**), three (**I**) and six (**J**) weeks post-loading. Yellow arrows indicate damage to the cartilage that was scored as OA-like. Images shown are 25x magnification with scale bars representing 200µm

Figure 3: Severity of synovitis following MJL

Ipsilateral and contralateral knees of 9N-loaded mice (red squares, n = 5-6) were collected post mortem at weeks one, three and six post-loading after which the severity of synovitis was scored for each joint section. Values were compared to non-loaded isoflurane controls (black circles, n = 5-6). Scoring system ranges from 0-6, synovitis is classified as either low (grade 0-2), mild (grade 3-4) or severe (grade 5-6). For each sample, maximum (**A**; ipsilateral knees, **B**; contralateral knees) and summed scores (**C**; ipsilateral knees, **D**; contralateral knees) are given. Differences in the severity of synovitis between groups are indicated with a * ($p < 0.05$), ** ($p < 0.01$) or *** ($p < 0.001$). Values given as mean ± SD.

Figure 4: Corticosterone levels in the fur of loaded and non-loaded mice after MJL

Fur of 9N-loaded mice (red squares, $n = 6$) and non-loaded isoflurane controls (black circles, $n = 6$) were collected post mortem at weeks one, three and six post-loading. The fur was processed and analysed to determine the corticosterone levels as a measure for chronic stress. Differences in corticosterone levels are indicated with a * ($p < 0.05$). Values given as mean ± SD.

Figure 5: Tyrosine hydroxylase (TH) and calcitonin gene-related peptide (CGRP) positive nerve fibres following MJL

Ipsilateral knees of 9N-loaded mice (red squares, $n = 5$) and non-loaded isoflurane controls (black circles, $n = 5$) were collected post mortem at weeks one, three and six post-loading. Knees were processed for nerve analysis after which the total volume of TH+ (**A**) and CGRP+ (**B**) nerve fibres were determined. There were no significant differences in total nerve volumes. Innervation of TH+ (**C**, **E**, **F**) and CGRP+ (**D**, **F**, **H**) nerve fibres in the respective compartments; lateral meniscus (LM), medial meniscus (MM), cruciate ligament (CM), the lateral collateral ligament (LCL), medial collateral ligament (MCL), and periosteum (P), is given as a volume at week one (**C**, **D**), three (**E**, **F**) and six (**H**, **I**) weeks post-loading. Values given as mean ± SD.

Figure 6: Visualization of TH+ and CGRP+ labelling in specified regions of the knee joint of loaded and non-loaded mice at week one following MJL

Innervation of the knee joint was imaged in coronal sections (**A**). Regions used to image are showed on toluidine blue stained section (**B**). Examples of typical nerve fibres expressing TH+ (**C**) and CGRP+ (**D**) are shown for the lateral collateral ligament, medial collateral ligament, cruciate ligament, lateral meniscus, medial meniscus and periosteum of loaded and non-loaded ipsilateral knees at week one post-loading. Images are shown at 40x magnification with scale bars representing 50µm.

Figure 7: Correlation analysis between pain behaviours and OA parameters following MJL

Overall correlation analysis (**A**) was run between parameters for OA-like severity of cartilage damage (green), nerve volume (violet), corticosterone levels (red), subchondral bone integrity (purple) or synovitis scoring (yellow) and nociceptive behaviour at weeks one, three and six post-loading. For each time point, differences between baseline and final behavioural thresholds (difference score) of the ipsilateral mechanical thresholds (50% PWT) and weight bearing values (% weight ipsilateral) were used as behavioural read-outs for the correlation analysis. Correlations range from -1 (dark blue; indicative of perfect negative correlation) to 1 (dark red; indicative of perfect positive correlation). Specific correlation between ipsilateral mechanical threshold difference scores plotted against the summed OA cartilage scores (**B**) is shown for loaded mice and non-loaded controls sacrificed at weeks one (orange dots, $n = 11$), three (blue dots, $n = 11$) and six (green dots, $n = 12$) post-loading. Linear trendlines and corresponding R2 values are portrayed on the graph.

Supplementary methods

Measurement of pain-associated behaviours

Both testing and holding environments were climate and light controlled; temperature 21°C, humidity 50%, lights on from 7AM-7PM. Animals arrived a week before baseline behavioural testing to allow for acclimatization. Procedures and behavioural tests were conducted during the light phase of the day-night cycle (8AM-6PM). Animals were trained and allowed to acclimatize to the behavioural testing set-up prior to the start of the experiment. Behavioural experiments were done in a separate room to ensure a quite environment during testing. Between the behavioural assays, mice were allowed a minimum of an hour rest. Researchers performing behavioural testing were blinded to the condition of the mice but not to the week of the experiment. For each behavioural assay the same researcher followed the animals for the duration of the experiment. Researchers conducting both the MJL to induce OA and the following behavioural testing were female. Mice were assigned conditions in a pseudo-random order based on behavioural baseline values. In this, there was an even spread of high and low responders over different experimental groups thus ensuring comparable behavioural baseline values between groups. Furthermore, care was taken to allocate different conditions within the home cage allowing for two loaded mice to be home-caged with two non-loaded mice. Furthermore, the comparability of baseline values minimizes the baseline effect in the use of the difference score (the difference between baseline and final behavioural thresholds) in the correlation analysis. Two mice, a non-loaded control sacrificed at week three post-loading and a loaded mouse sacrificed at week one post-loading, were excluded from analysis due to fighting wounds or faulty loading, respectively. Mice were sacrificed per time point in a randomized order based on cage number. Sample size was calculated based on expected ipsilateral mechanical hypersensitivity read-out for both loaded and non-loaded at weeks 1, 3 and 6 in previously published data [1]. Specifically, means used for the sample size calculation at the three time points were 0.38, 0.20 and 0.13 for loaded animals, and 0.30, 0.49 and 0.60 for non-loaded animals; standard deviation was assumed to be 0.14 after pooling the data. Using a repeated measures design with a α value of 0.05 and power of 0.8, the required sample size was 5 per group (https://glimmpse.samplesizeshop.org/). Sample size of 6 per group was decided for the study to account for potential drop out.

Mechanical hyperalgesia

Mechanical allodynia, defined as the sensitivity to innocuous stimulus, was assessed by measuring touch perception thresholds with nylon von Frey microfilaments (Bioseb, Vitrolles, France). A set of von Frey filament weights ranging from 0.04g to 2g were used to apply pressure to plantar surface of

the paw. The up-down method was employed for obtaining 50% paw withdrawal threshold [2, 3]. Briefly; the 0.4g filament was always used to start the sequence; if a positive response was observed, a filament of a lesser weight would be used whilst if no response was observed then a filament of a higher weight would be employed. This stimulus was repeated 5 times after the first change in response. Flinching, biting, or paw withdrawal during or immediately after applying the stimulus are considered nociceptive defensive behaviours and were noted as positive responses. Mechanical sensitivity thresholds were measured in both hind paws; ipsilateral paw measurements would be taken first, then animals would be allowed a 30-minute rest after which the contralateral paw would be measured.

Weight bearing asymmetry

Static weight bearing was used to assess the amount of weight borne on the ipsilateral leg, a reduction of weight borne on affected limb being indicative of increased nociception [4]. Mice were positioned on an incapacitance meter (Linton Incapacitance Tester, UK) consisting of two scales with each hind limb placed on one of the scales and front limbs resting on the holding chamber. Once mice were still and resting, weight placed on each of the scales was measured for 5 seconds. Measurements were taken in triplicate allowing for the mice to readjust between measurements. Weight-bearing ratio, weight placed on affected limb divided by the total weight placed on both hind limbs, was calculated for each trial and then averaged per time point.

Post-mortem analyses

Microcomputed tomography analysis of subchondral bone integrity

High resolution microcomputed tomography (µCT) was used to asses trabecular and cortical bone morphology of the subchondral bone. Following sacrifice, hindlimbs were dissected out, placed in 4% neutral buffered formalin and allowed to fix for 48 hours at 4°C. Samples were then stored in 70% IMS at 4°C until µCT scanning could be performed. Scanning was performed at a resolution of 5 µm/pixel using the µCT scanner (Skyscan 1172; Bruker, Kontich, Belgium) with the following settings; 0.5mm aluminium filter, medium camera (2000 x 1336 pixels), 50kV voltage, 200µA current, 0.6° rotation and a 2-frame averaging. Imaging data from µCT scans was reconstructed with NReconstruction (NRecon, version 1.7.1.0; Bruker). For analysis of the subchondral bone of the tibia scans were reoriented using Dataviewer (Dataviewer, version 1.5.2.4; Bruker) with the tibial growth plate of the tibia aligned parallel to the transversal plane and the tibia aligned straight in the sagittal plane. For analysis of the subchondral bone of the femur scans were reoriented again to allow for alignment of the growth plate of the femur parallel to the transversal plane with the femur aligned straight in the sagittal plane.

The coronal view was used to select regions of interest in CTAnalyser (CTAn, version 1.17.7.1 +; Bruker). Subchondral bone integrity was analysed in the posterior compartments of both tibia and femur. The begin-point for the tibia was identified by the anatomical landmark where the condyle cleft begins to form, and the ossified menisci start to appear, and the end-point identified as the point where the condyles are no longer connected (245 slices ± 5 slices per joint for analysis). For the femur the begin-point was identified as the point where ossified meniscus become visible and the end-point as the point where clearly shaped trabecular bone was no longer visible (210 slices ± 5 slices per joint for analysis). Subsequently, regions of interest (ROI) were selected using the free-hand contouring method to separate trabecular and cortical bone. Firstly, trabecular bone was selected parallel to the endocortical boundary, staying above the growth plate. Then, in a data set omitting the trabecular bone, the subchondral cortical bone was selected from the medial to lateral boundary.

Hitsomophometric analysis was performed with the 2D and 3D analysis program Batman (BATMAN, version 1.14.4.1; Bruker). Global thresholding (scale: 0 – 225) for bone was set at a low value of 70 and a high value of 225. White speckles smaller than 20µm were removed in 2D and 3D space. For trabecular analysis, ROI volumes were loaded together with the scan data to allow for tissue volume analysis. Parameters analysed are given in

Table 2.

Table 2: Output parameters for subchondral bone morphology.

Parameter	Description	Abbreviation (unit)
3D analysis		
Bone volume percentage	The ratio of segmented bone volume to total volume of ROI	BV / TV (%)
2D analysis		
Trabecular cross-sectional thickness	Mean thickness of trabeculae diameter	Tb.Th (mm)
Cortical plate thickness	Mean cross-sectional cortical thickness	Cs.Th (mm)

Histological analysis of OA pathology

Samples were decalcified in immunocal (Quartett, Berlin, Germany) for 5 days at room temperature under constant rotation. Decalcification progression was checked daily and verified using the µCT. Following decalcification, samples were processed for paraffin embedding (Vacuum Infiltration Processor; Tissue Trek VIP, Sakura, USA) to allow for coronal sectioning with the patella of the knee facing downwards to the cutting surface. Coronal sequential sections of 6µm were taken from the entire joint (approximately 250 sections in total). Four sections were placed on each consecutive slide (SuperFrost Plus™ Adhesion slides; Thermo Fisher Scientific). Each fourth slide (12th-16th section) was stained with toluidine blue (0.1% in 0.1M acetate buffer pH 5.6; Sigma-Aldrich) and used to grade OA and synovitis severity. Knee sections were divided in 4 compartments and severity of articular cartilage lesions or synovitis was scored for each condyle; lateral and medial, femur and tibia.

Cartilage grading: Severity of OA-like lesions in the cartilage was scored for each stained section using a grading system [5] ranging from 0-6. Briefly, grade 0 corresponds to normal surface articular cartilage; grade 0.5, a loss of toluidine blue staining; grade 1, lesions in the superficial zone of the articular cartilage; grade 2, lesions down to the intermediate zone; grade 3, lesions down to the tidemark with possible loss of articular cartilage up to 20% of the surface of the condyle; grade 4, loss of 20% to 50% articular cartilage; grade 5 loss of 50-80% of articular cartilage; and finally, grade 6, with above 80% articular cartilage loss and exposure of subchondral bone. For each sample maximal OA score, determined as the lesion with the highest severity, and summed OA score were given. OA severity is classified as either low (grade 0-2), mild (grade 3-4) or severe (grade 5-6).

Synovitis grading: The six-point grading system as described by Lewis and colleagues [6] was used to score the severity of synovitis in each sample. Synovial pathology was scored at the insertion of the synovial lining at the femur and tibia. Changes in synovial lining thickness were scored ranging from 0 to 3 with grade 0 representing a single cell layer thickness, grade 1 a cell layer thickness of 2-4 cells, grade 2 a cell layer thickness of 4-8 cells and finally grade 3 representing a cell layer of more than 8 cells. Cellular density in the synovial stroma was scored separately on a scale from 0 to 3. Grade 0 represented normal cellularity in the synovial stroma, grade 1 a slightly increased cellularity, grade 2 moderately increased cellularity and grade 3 a greatly increased cellularity with pannus and granuloma formation. The scores for synovial lining and cellular density were then combined to give a single score of synovitis severity. For each sample the maximal score, determined as the lesion with the highest severity, and summed OA score were given.

Nerve analysis

Immunocytochemistry was used to identify sensory and sympathetic nerves (in accordance with published literature [7]) in the knee joint which were then quantified to determine the influence of MJL-induced OA on nerve volume. To aid preservation of the nerves, samples were collected using perfusion fixation in mice [8]. Transcardial perfusion was performed first using heparinised 0.01M phosphate buffered saline (1 I.U./mL heparin sodium (Wockhardt, Mumbai, India) in 20 mL 0.01M PBS, pH 7.4) and a picric acid fixative solution (20 mL 12.5 % picric with 4% paraformaldehyde in 0.01M PBS, pH 6.9; Sigma-Aldrich). Following dissection, samples were placed in the picric acid fixative solution and stored for 48 hours at 4°C to ensure adequate fixation. Once fixated, samples were washed three times in 0.01M PBS and then placed in 10% ethylenediaminetetraacetic acid (EDTA; Sigma-Aldrich) in 0.01 M PBS to decalcify for seven to ten days at 4°C. Complete decalcification was tracked using µCT imaging. As soon as complete decalcification was confirmed, samples were placed in 30% sucrose solution (Sigma-Aldrich) to cryoprotect the tissue. They were stored in sucrose solution at 4°C for a minimum of 48 hours to ensure tissues saturation after which they were frozen and stored at -20°C until further processing.

Sample sectioning was done on the same day the immunocytochemistry staining took place to minimize nerve degradation. Samples were embedded in optimal cutting temperature media (OCT; Sakura, California, USA) in the same orientation as used for the histological analysis to enable comparison between OA scoring and nerve localization. Coronal sections of 30µm were cut and collected on slides. Sensory and sympathetic nerves were labelled with primary antibodies against calcitonin gene-related peptide (CGRP) and tyrosine hydroxylase (TH), respectively. In both cases Cynanine 2 (Cy2) was used as a secondary antibody. To label large nuclei on the sections 4′,6-diamidino-2-phenylindole (DAPI) was used as a counterstain (see Table 3 an overview of the antibodies and their dilutions).

Stained sections of the knee joint were imaged in six locations; the lateral and medial collateral ligament attachment at the femur, the lateral and medial meniscus, the cruciate ligament and the periosteum of the tibia. These regions were chosen in accordance with their anatomical importance for nerve in-growth during knee inflammation [9, 10]. Slides were imaged used Leica SP5 confocal microscope with Leica Application Suite advanced fluorescence software (Leica Application Suite, version 2.6; Leica Microsystems), equipped with a 405 nm diode laser to identify DAPI. For both the CRGP and TH nerve markers a confocal Z-stack of images at 1µm increments was taken at each region of interest. Z-stacks were taken at 10x (10x HCX PL FLUOTAR PH1; NA = 0.3) and 40x (40x HCX PL FLUOTAR PH1; NA = 0.75) magnifications.

After imaging, the CGRP+ sensory and TH+ sympathetic nerve volumes were determined automatically using a thresholding method in an imaging analysis program (Volocity, version 6.3; PerkinElmer, Massachusetts, USA). All images analysed this way were acquired using the same settings (at 40x magnification). Low and high thresholds for the Cy2 marker were set to 35 and 255, respectively with any objects smaller than 2µm^3 being excluded from analysis. This thresholding range ensured all Cy2 labelled tissues, identified as nerves, were quantified.

Table 3 Overview of antibodies and their dilutions used for immunocytochemistry.

Labelling target	Antibody	Dilution	Supplier
Primary antibodies			
calcitonin gene related peptide (CGRP)-rich sensory nerves	Rabbit Anti-CGRP	1:5,000	Sigma-Aldrich, Missouri, USA
tyrosine hydroxylase (TH)-rich sympathetic nerves	Rabbit Anti-TH	1:1,000	Merck Millipore, Massachusetts, USA
Secondary antibody			
Rabbit	Goat Anti-Rabbit Cyanine 2 (Cy2) labelled	1:200	Jackson ImmunoResearch, Pennsylvania, USA
Counter stain			
Large nuclei	4′,6-diamidino-2-phenylindole (DAPI)	1:20,000	Sigma-Aldrich, Missouri, USA

Analysis of corticosterone levels in mice fur

Fur samples were taken post-mortem from the mice flanks. Fur was wiped down using demineralized water to minimize potential contamination of hair from cage mates after which fur was removed from as closely to the skin as possible using scissors and tweezers. Fur was transferred into 1,5mL Eppendorf tubes with stainless steel ball bearings. Tubes containing fur were then placed in a tissue homogeniser (Retsch Tissue Homogeniser Mixer Mill MM300) and each sample was ground for 30 minutes at 30Hz until fur was pulverized, weighed and then transferred to glass vials. Corticosterone was extracted by adding 2mL of methanol to the glass vials that were allowed to incubate for 18 hours at 37ºC on slow rotation. After extraction, 1,5mL of the methanol was transferred into clean 2mL Eppendorf tubes. These tubes were centrifuged at 10000G for 10 minutes at 4ºC and supernatant was transferred to get rid of any residue. Samples were dried using a centrivap concentrator (Labconco) under 2 bar pressure at 60ºC for 5 hours to evaporate methanol. Dry extract was then dissolved in 200µL assay buffer supplied by the corticosterone enzyme immunoassay kit and diluted at 1:50. Corticosterone levels in diluted samples were quantified using a commercially available ELISA kit (Corticosterone ELISA Kit, Item Number 501320, Cayman Chemical, Michigan, USA). Assay was developed in the dark during continuous shaking for 120min. It was read on a plate reader (DLReady, Mithras LB940) after 90 and 120 minutes at an absorbance level of 450nm. Output values of pg/mL were corrected for amount of fur and expressed as ng/mL/mg. In order to prevent any effects of inter-assay variability all samples that were statistically compared were run in the same assay; intra-assay coefficient of variance was less than 3%.

References

1. Ter Heegde, F., et al., *Non-invasive mechanical joint loading as an alternative model for osteoarthritic pain.* Arthritis Rheumatol, 2019.
2. Bonin, R.P., C. Bories, and Y. De Koninck, *A simplified up-down method (SUDO) for measuring mechanical nociception in rodents using von Frey filaments.* Mol Pain, 2014. **10**: p. 26.
3. Chaplan, S.R., et al., *Quantitative assessment of tactile allodynia in the rat paw.* J Neurosci Methods, 1994. **53**(1): p. 55-63.
4. Malfait, A.M., C.B. Little, and J.J. McDougall, *A commentary on modelling osteoarthritis pain in small animals.* Osteoarthritis Cartilage, 2013. **21**(9): p. 1316-26.
5. Glasson, S.S., et al., *The OARSI histopathology initiative - recommendations for histological assessments of osteoarthritis in the mouse.* Osteoarthritis Cartilage, 2010. **18 Suppl 3**: p. S17-23.
6. Lewis, J.S., et al., *Acute joint pathology and synovial inflammation is associated with increased intra-articular fracture severity in the mouse knee.* Osteoarthritis Cartilage, 2011. **19**(7): p. 864-73.
7. Chartier, S.R., et al., *Exuberant sprouting of sensory and sympathetic nerve fibers in nonhealed bone fractures and the generation and maintenance of chronic skeletal pain.* Pain, 2014. **155**(11): p. 2323-36.
8. Gage, G.J., D.R. Kipke, and W. Shain, *Whole animal perfusion fixation for rodents.* J Vis Exp, 2012(65).
9. Ghilardi, J.R., et al., *Neuroplasticity of sensory and sympathetic nerve fibers in a mouse model of a painful arthritic joint.* Arthritis Rheum, 2012. **64**(7): p. 2223-32.
10. Jimenez-Andrade, J.M. and P.W. Mantyh, *Sensory and sympathetic nerve fibers undergo sprouting and neuroma formation in the painful arthritic joint of geriatric mice.* Arthritis Res Ther, 2012. **14**(3): p. R101.

Supplementary results

Table 4 Individual correlation values per OA pathology parameter tested

OA pathology parameters	One week post-loading		Three weeks post-loading		Six weeks post-loading	
	Difference score 50% PWT	**Difference score weight bearing**	**Difference score 50% PWT**	**Difference score weight bearing**	**Difference score 50% PWT**	**Difference score weight bearing**
Maximum OA score	0.076447	0.53513	0.748347	0.410857	0.784749	0.700299
Summed OA score	0.237273	0.279145	0.478193	0.220704	0.728646	0.676264
Total volume CGRP+ nerves	-0.26061	0.50303	0.260606	0.163636	-0.34545	0.236364
Total volume TH+ nerves	-0.05455	0.260606	-0.04242	0.490909	-0.39394	0.175758
Corticosterone	0.333333	0.213235	0.006993	0.048951	0.216783	-0.00699
Cortical crossectional thickness tibia	0.472727	-0.24545	0.687929	0.583145	0.042106	0.111888
Cortical bone volume tibia	0.136364	-0.16364	0.645455	0.754545	-0.0386	-0.00699
Trabecular crossectional thickness tibia	0.036364	0.572727	0.736364	0.581818	-0.29474	0.048951
Trabecular bone volume percentage tibia	-0.01818	0.536364	0.781818	0.636364	-0.34737	-0.04895
Cortical crossectional thickness femur	-0.18182	0.609091	-0.07273	-0.52727	0.343862	0.314685
Cortical bone volume femur	-0.33636	0.381818	0.545455	0.163636	0.368423	0.244755
Trabecular crossectional thickness femur	0.036364	0.363636	0.727273	0.463636	-0.04561	0.195804
Trabecular bone volume percentage femur	0.209091	0.363636	0.718182	0.418182	-0.32632	-0.02797
Maximum synovitis score	0.145266	0.276475	0.731988	0.43823	0.63295	0.197104
Summed synovitis score	-0.0046	0.372438	0.710708	0.55581	0.624129	0.201425

Table 5 Corresponding p-values for correlation analysis per OA pathology parameter tested

OA pathology parameters	One week post-loading		Three weeks post-loading		Six weeks post-loading	
	Difference score 50% PWT	Difference score weight bearing	Difference score 50% PWT	Difference score weight bearing	Difference score 50% PWT	Difference score weight bearing
Maximum OA score	0.823223	0.089833	0.008068	0.209385	0.002503	0.011208
Summed OA score	0.48236	0.405816	0.136809	0.514307	0.00719	0.015752
Total volume CGRP+ nerves	0.467089	0.138334	0.467089	0.651477	0.328227	0.510885
Total volume TH+ nerves	0.881036	0.467089	0.907364	0.149656	0.259998	0.627188
Corticosterone	0.191058	0.411226	0.982792	0.879919	0.498556	0.982792
Cortical crossectional thickness tibia	0.141999	0.466922	0.019291	0.059696	0.896625	0.729195
Cortical bone volume tibia	0.689309	0.630685	0.031963	0.007282	0.905204	0.982792
Trabecular crossectional thickness tibia	0.915468	0.065543	0.00976	0.06042	0.352379	0.879919
Trabecular bone volume percentage tibia	0.957685	0.088953	0.004473	0.035287	0.268581	0.879919
Cortical crossectional thickness femur	0.592615	0.046696	0.831716	0.095565	0.273772	0.319139
Cortical bone volume femur	0.311824	0.24656	0.082651	0.630685	0.238639	0.443262
Trabecular crossectional thickness femur	0.915468	0.271638	0.011205	0.150901	0.888057	0.541936
Trabecular bone volume percentage femur	0.537221	0.271638	0.0128	0.20057	0.300583	0.931234
Maximum synovitis score	0.669985	0.41051	0.010437	0.177598	0.027165	0.539203
Summed synovitis score	0.989295	0.259325	0.014228	0.075842	0.030073	0.530161

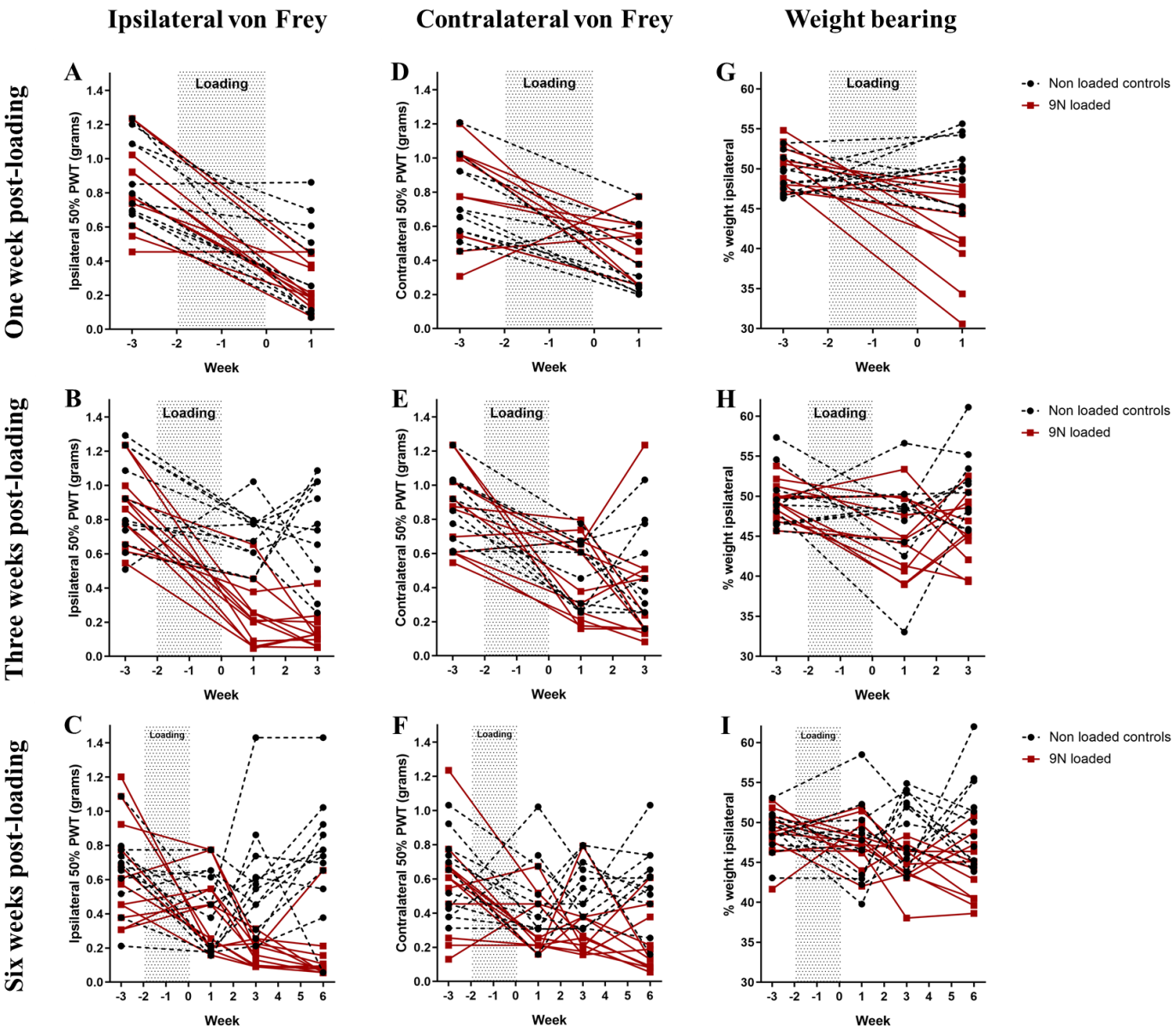

Figure 8 Development of mechanical hypersensitivity and altered weight bearing following MJL presented as individual values

Individual behaviour read-outs of 9N loaded mice (red line, n = 12 per time point) compared to non-loaded isoflurane controls (black dotted line, n = 12 per time point) at weeks one (**A**, **D**, **G**), three (**B**, **E**, **H**) and six (**C**, **F**, **I**) post-loading. Development of mechanical hypersensitivity was measured using von Frey filaments (50% paw withdrawal threshold (PWT) in grams) in the ipsilateral (**A**, **B**, **C**) and contralateral (**D**, **E**, **F**) paws. Altered weight bearing (weight placed on ipsilateral paw as a percentage of total weight placed on both legs) was measured using the incapacitance test (**G**, **H**, **I**).

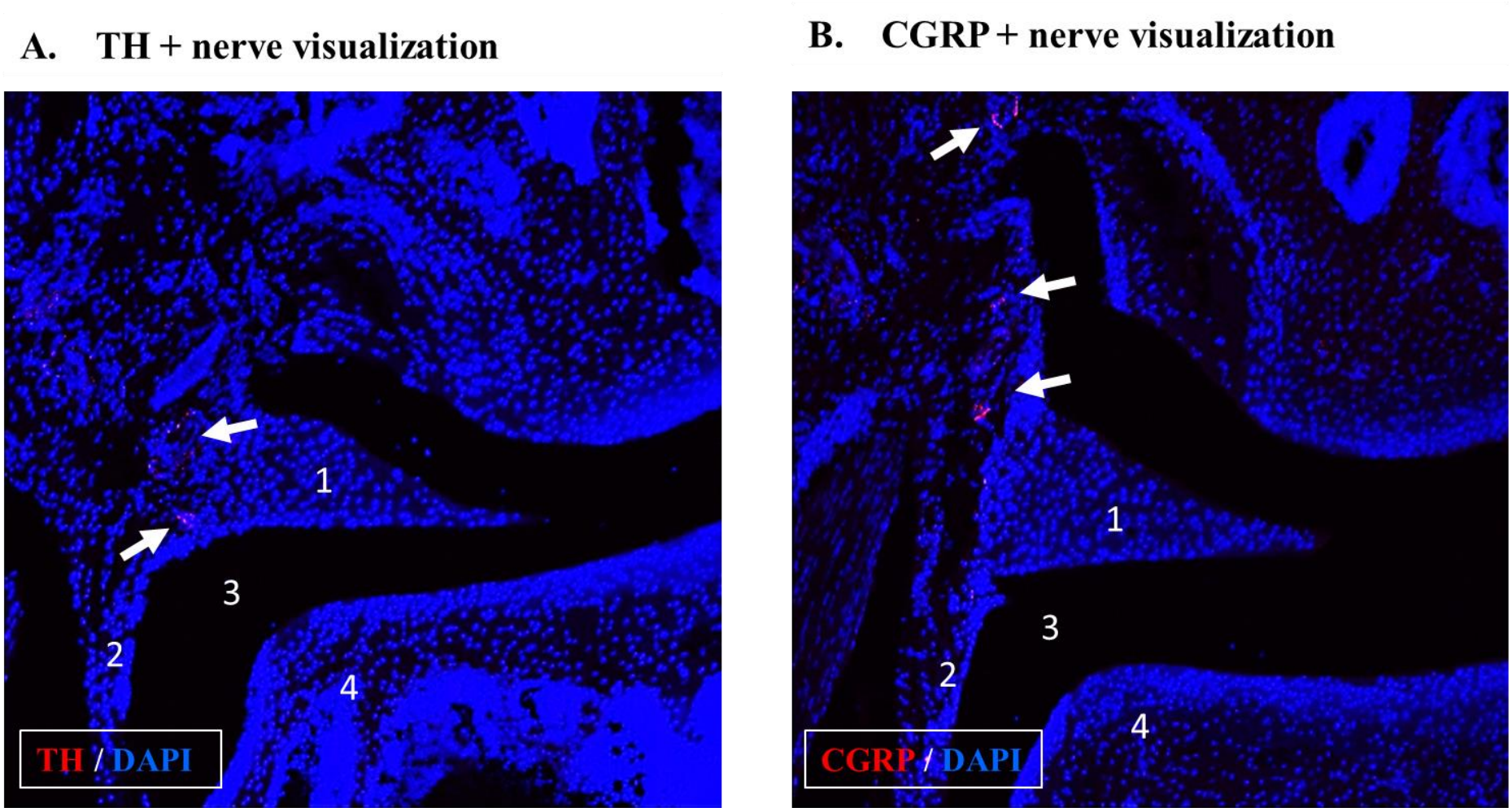

Figure 9 : Higher magnification visualization of TH+ and CGRP+ expression in subchondral bone and synovium of the knee joint of loaded mice at week one following MJL.

Examples of typical nerve fibres expressing TH+ (**A**) and CGRP+ (**B**) are shown for the meniscus (1), synovial lining (2), synovium (3) and subchondral bone (4) in loaded ipsilateral knees at week one post-loading. Images are shown at 10x magnification, arrows indicate innervation seen in collateral ligaments and meniscus.